April 2017

Investigating a novel Cu+ storage protein in Pseudomonas aeruginosa

Andrew Steven Baez
Worcester Polytechnic Institute

JMA MQP

Investigating a novel Cu^{+} storage protein in *Pseudomonas aeruginosa*

Submitted to the Faculty

of

Worcester Polytechnic Institute

in partial fulfillment of the requirements for a

Degree of Bachelor of Science

by

Andrew Baez

Date: April 21, 2017

Approved:

Professor José M. Argüello

Biochemistry

WPI Project Advisor

Abstract

Cu^{+} is a vital element for cellular functions as it is a cofactor for many essential enzymes. However, at high concentrations, it can be toxic to the cell due to its ability to perform Fenton-like chemistry. Therefore, cells need to tightly control the amount of intracellular Cu^{+1} by either exporting it out of the cell or storing it in a protein. Recently, a small secreted protein with high Cu^{+1} binding capability, Csp1, has been identified in the methanotroph *Methylosinus trichosporium OB3b.* In this work, its homologue in *Pseudomonas aeruginosa* was studied. This organism is an opportunistic pathogen in plants and animals that is commonly found in hospital infections. To understand its role in *P. aeruginosa*, the construction of expression and mutant/complemented strains of the *csp1* gene was attempted. In addition, the transcriptional levels of *csp1* in response to Cu^{+1} and related stress conditions was tested using RT-qPCR analyses. The results showed that the transcriptional levels of the *csp1* gene remained constant under Cu^{+1} toxic levels, suggesting Csp1 might not play a role in Cu^{+1} detoxification.

Acknowledgments

I would like to thank Professor José Argüello for his invaluable insight and direction throughout this project and for giving me the opportunity to work in a research laboratory during my 4 years of undergraduate studies. I also want to thank Julia Quintana González for helping me an incalculable amount of times throughout the year. Additionally, I would like to thank Lorena Novoa-Aponte, and Robert McNeilage for allowing me to work alongside them and for their constant support. This work was supported by NIH grant R01 GM114949 to Prof. José Argüello.

Table of Contents

Table of Figures

I. Introduction

Transition metals are part of our daily life, since they are ever present in "domestic, agricultural, medical and technological applications" (1). Some of those elements participate in key biochemical process such as O_2 transport, redox reactions and protein synthesis, among others (2). Cells should act to guaranty metal availability while preventing deleterious effects of over accumulation.

Cu^+ is a critical cofactor for the function of several enzymes in eukaryotic and prokaryotic organisms. The binding of Cu^+ to the active site of some proteins involved in aerobic respiration is required for their function. Examples include; Super Oxide Dismutase (SOD), which plays a role in converting O^-_2 radicals to O_2 or H_2O_2; and Cytochrome c Oxidase which plays a role in the electron transport chain of mitochondria (3,4).

At the core of Cu^+ roles in biological systems is its ability to cycle between two oxidative states. This characteristic makes it a versatile ion; nonetheless, over accumulation of the reduced form of this metal can lead to toxicity (5). Through Fenton-like chemistry Cu^+ produces highly reactive O_2 radicals in the cytosol, which generates deleterious effects to the cell. This phenomenon forces the cell to devise mechanisms to maintain where low cytosolic Cu^{+1} levels, where there is no free intracellular Cu^{+1} (6).

Cu^+ homeostasis mechanism are thus very important for survival in biological organisms. Impaired Cu^+ homeostasis in humans has been linked to Menkes' and Wilson's diseases. Menkes' disease is an X-linked recessive disorder that is caused by Cu^+ deficiency, while Wilson's disease is autosomal recessive disorder that is caused by Cu^+ accumulation (7). Both diseases are caused by mutations in P-type Cu^+ ATPases, involved in Cu^+ transport; Menkes' by a mutation in ATP7A, an importer, and Wilson's diseases by a mutation in ATP7B, an exporter (8-10).

Studies on bacterial Cu^{+} homeostasis have mainly focused on membrane and periplasmic mechanisms of bacterial tolerance to Cu^{+1} overload (11,12). These have revealed the existence of various Cu^{+1} related elements: transcriptional regulators, soluble chaperones, and membrane transporters (13). However, distribution systems that place the metal in target cupro-enzymes, sensors, and storage proteins are likely to participate in Cu^{+} homeostasis.

A plethora of efflux and chaperon systems for Cu^{+1} have been discovered, characterized or proposed in bacteria (summarized in Fig. 1). It is hypothesized that Cu^{+2} import to the cytoplasm of bacteria is probably achieved through major facilitator superfamily of transport proteins (14). Once inside the cytoplasm multiple metallo-chaperones, such as CopZ, direct the incoming Cu^{+1} to its target enzyme or transcriptional regulator (15). In the case of CopZ, it can be hypothesized that it delivers Cu^{+} to the one of two $P_{1\text{-}B}$ ATPases, CopA1 or CopA2. Through CopA1, Cu^{+1} is transported out of the cytoplasm to the periplasm of the cell where it is then directed to an efflux system for detoxification. Meanwhile, it has been proposed that CopA2, although highly homologous to CopA1, does not play a role in detoxification, but that it aids in the metallation of cuproproteins in the periplasm (12,16). It has been suggested that CopA2 helps in the formation of cytochrome oxidases, as it is co-transcribed with two cytochrome oxidase subunits (12). Interestingly, the rate of transport of both enzymes is related to its functional diversity; CopA2 displays lower rate compared to CopA1 (16).

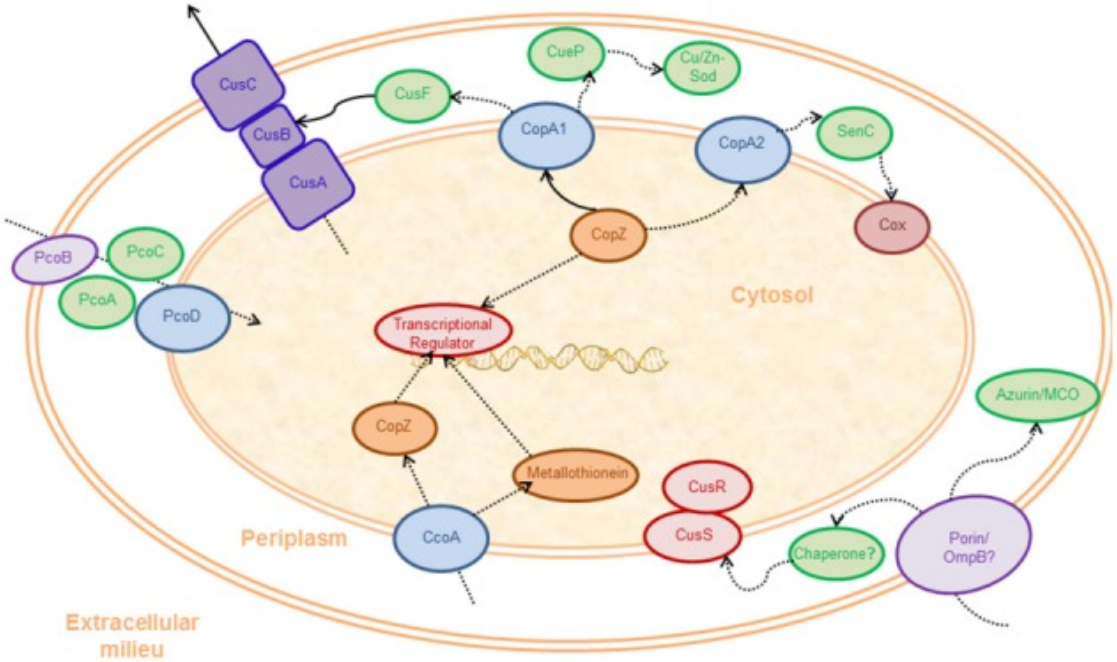

Figure 1: Hypothesized Cu^{+} homeostasis for Pseudomonas Aeruginosa

The Cu^{+} homeostasis model shown in Figure 1 has been proposed for the opportunistic pathogen *Pseudomonas aeruginosa. P. aeruginosa, a gram-negative bacterium,* cell possess an outer-membrane, a periplasmic space, an inner-membrane and the cytoplasm. The outer-membrane's low permeability plays a big role in providing antibiotic resistance, as it restricts the ability of antimicrobial peptides to create stochastic holes in the bacteria, which enable bacterial uptake of antibiotics (17). This phenomenon allows *P. aeruginosa* to adapt to an array of environments. This organism is accredited for nearly 10% of infections acquired in hospitals around the world (18,19). Recently, the World Health Organization recognized *P. aeruginosa* as one of the three most critical pathogens with a need of antibiotic development (20). This creates a clear need to further our understanding on the mechanisms behind its increased resistance to harmful environments. In this regard, it has been shown that the deletion of P-type Cu^{+1} ATPases lead to decreased virulence of *P. aeruginosa* (12). These transporters extrude excess Cu^{+1} from the cytosol to the periplasm in gram-negative bacteria and to the extracellular milieu in gram-positive

bacteria (13,21). However, this is not an immediate response. We hypothesize that a pool of storage proteins might serve as a fast response to Cu^{+1} overload.

In eukaryotes excess of Cu^{+1} is stored cysteine-rich in metallothioneins (22). Cysteine is one of the few amino acids capable of forming covalent bonds through its thiol side chain with metal ions. In oxidizing environments, the thiol group loses its hydrogen making it a likely binding partner to transition metals like Cu^{+} (23). Intriguingly, most prokaryotic organisms are thought not to contain Cu^{+1} storage proteins. Nonetheless, a Cu^{+1} binding metallothionein, MymT, which plays a role in Cu^{+1} detoxification has been identified in *Mycobacterium tuberculosis*(24). MymT is a cysteine rich protein that is capable of binding 6 Cu^{+1} ions. Interestingly, *MymT* expression was induced by Cu^{+1}, cadmium and under oxidative stress. More recently, a secreted copper storage protein (Csp1) was described in *Methylosinus trichosporium* (25). Csp1 is a cysteine-rich protein, with 13 cys per monomer. Its functional form is a tetramer capable of storing 52 Cu^{+1} ions (Fig. 2). In methanotrophs it has been proposed that Csp1 plays a role in providing Cu^{+1} for methane oxidation (25).

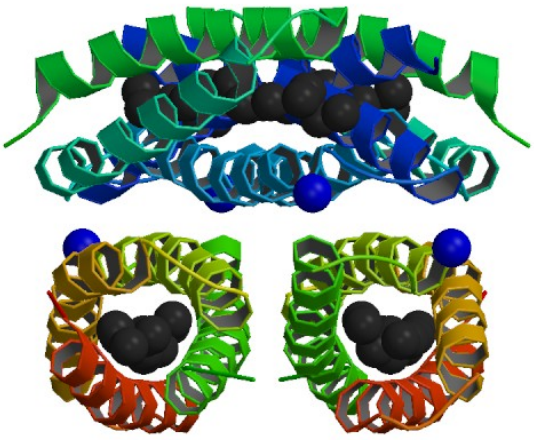

Figure 2: Crystal structure of Csp1 in *Methylosinus trichosporium OB3b* (24).

A cytosolic Csp1 homologue is present in *P. aeruginosa* (PA2107). The sequence alignment of the *csp1* genes of *P. aeruginosa and M. trichosporium* shows that cysteine residues are fully conserved (Fig. 3), suggesting a similar role in Cu^{+} homeostasis. We hypothesize that Csp1 might act as a Cu^{+} buffer in an early response to Cu^{+1} stress. The main goal of this project was to investigate the role in Cu^{+} homeostasis of the Csp1 orthologue of *P. aeruginosa*.

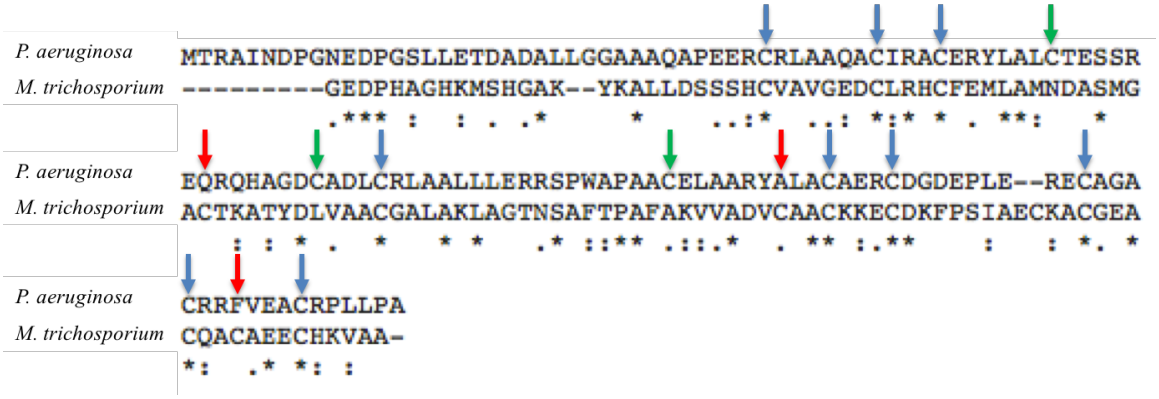

Figure 3: Homology between Csp1 from *Pseudomonas aeruginosa* and *Methylosinus trichosporium* OB3b. Blue arrows indicate cysteine residues that are conserved, green arrows show cysteine residues that are only present in *P.aeruginosa* and red arrows denote cysteine residues that are only present in *M. trichosporium* OB3b.

II. Methods

Cloning of the csp1 gene*: Csp1* gene sequence from *P. aeruginosa* PAO1 strain was obtained from the Pseudomonas Genome Database (26). The gene was amplified through PCR using the primers in Table 1. Denaturation was performed at 95 ^{o}C for 30 s, followed by an annealing step at 55 ºC for 30 s and an elongation at 72 ºC for 30 s. This cycle was repeated 25 times, followed by a final elongation step at 72 ºC for 30 s. Each PCR reaction was performed in a 50 uL reaction volume containing 0.5 mM of each primer, 0.5 mM dNTP mix, 5X Q5 Polymerase Buffer (New England Bio Labs), Q5 Polymerase(1U/1µL) (New England Bio Labs) and 100 ng of genomic PAO1 WT DNA as a template. The amplification of the gene was verified in 1% agarose gel electrophoresis, using 100 bp ladder (New England Bio Labs).

The PCR fragment containing the *csp1* gene was cloned into the pBAD TOPO-TA expression vector (Invitrogen) (Fig. 4). Adenine overhangs were added to the PCR product for gene insertion by incubating it for 20 min at 72 ^{o}C with 0.2 mM dATPs, 10x Taq Polymerase Buffer (New England Bio Labs), and One Taq Polymerase(1U/1uL) (New England Bio Labs). The plasmid was propagated in *Escherichia coli* Top10 cells and the protein expression was done in *E. coli* LMG194 cells (Invitrogen). For the transformation, 1 µL of plasmid was added to both cell types and incubated in ice for 30 min. These were heat shocked at 42 ^{o}C for 45 s, after which 500 µL of LB media was added. Cells were incubated at 37 ^{o}C for 1h, and 100 µL aliquots were plated on LB + 100 µg/ml ampicillin plates.

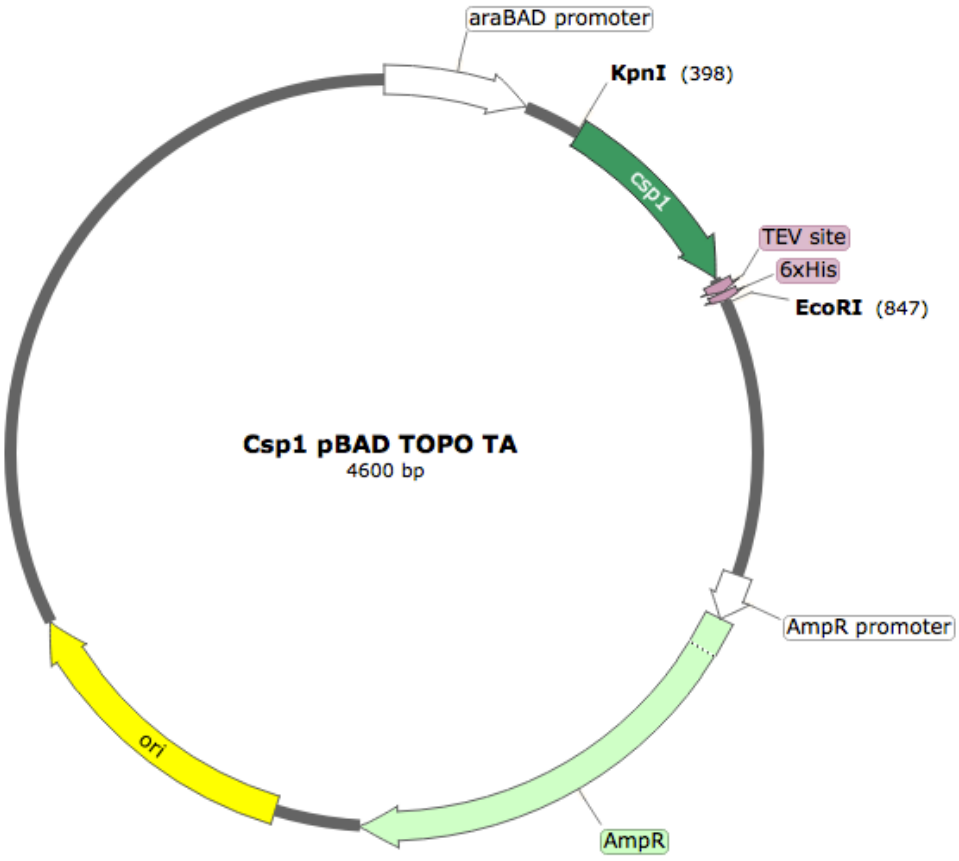

Figure 3: Csp1 pBAD TOPO TA expression vector map. Including the restriction digest sites, the ampicillin resistance gene, the arabinose promoter, origin of replication, 6x Histidine tag and TEV cleavage site.

Colonies were picked and suspended in 10 µL of H_2O, and boiled at 95 ^oC for 5 min. Correct insertions of the gene in the vector were tested by PCR using the cell lysates as template. Positive colonies were grown overnight in LB + ampicillin broth (10 g/l tryptone, 5 g/l yeast extract, 10 g/l NaCl, and 100 µg/ml ampicillin). Plasmids were isolated using the Qiagen kit. Plamids were verified by restriction digest with 800ng of purified DNA, 1 µL of each restriction enzyme (Kpn I and Eco-RI) (New England Bio Labs) and 1 µL of Cut Smart Buffer (New England Bio Labs). These products were run in a 1% agarose gel alongside an undigested plasmid, a partially digested plasmid and a 1kb DNA ladder (New England Bio Labs). Finally, the sequence of the clone was verified by automated sequencing.

Table 1: Primers used to create *csp1* expression vector.

Primer	Sequence (5'-3')
E-Kpn1-Csp1-F	GCATTAGGTACCATGACCCGCGCCATCAACGA
E-EcoR1-Csp1-R	TATAGGAATTCTCAGTGGTGGTGGTGGTGGTGG GACTGAAAATACAGGTTTTCGGCAGCAGCGGCC GGCAACAACGGCCGAC

Plasmid to generate a csp1 mutant strain: A 361 bp region located in the center of the *csp1* gene from *P. aeruginosa* PAO1 strain was amplified through PCR using the primers in Table 2. To create a vector capable of creating a mutant the pCHESIΩKm vector was used (27). The pCHESIΩKm vector was derived from the pUC18 family and includes a kanamycin resistance gene. The PCR product alongside with the pCHESIΩKm vector were digested for 1h at 37 ºC with XbaI and KpnI (New England Bio Labs). The digested product was then dephosphorylated utilizing shrimp alkaline phosphatase (1 unit/ug DNA) (Promega). The dephosphorylated PCR product and vector were then ligated and transformed following the protocol described above into *E. coli* Top 10 cells and S17.1 cells (Invitrogen).

Table 2: Primers used to create *csp1* mutant vector.

Primer	Sequence (5'-3')
M-KpnI-Csp1-F	GCATTAGGTACCATGACCCGCGCCATCAACGA
M-XbaI-Csp1-R	GCATTATCTAGAGCACATTCGCGCTCCAGCGG

Plasmid to complement the mutant strain: The coding sequence of the *csp1* gene and a region of 461bp upstream of the *csp1* start codon was amplified by PCR using *P. aeruginosa* PAO1 genomic DNA as template and the primers listed in Table 3. The PCR product was cloned in the *PUC18T-*

miniTN7T-Gm vector (28) (Fig. 5). The PCR product and the *PUC18T-miniTN7T-Gm* vector were digested for 1h at 37 ºC with SpeI and PstI (New England Bio Labs). The digested vector was the dephosphorylated utilizing shrimp alkaline phosphatase (1unit/ug DNA) (Promega) and then the PCR product was ligated into the vector. Ligated vectors were transformed into *E. coli* Top 10 and S17.1 cells (Invitrogen).

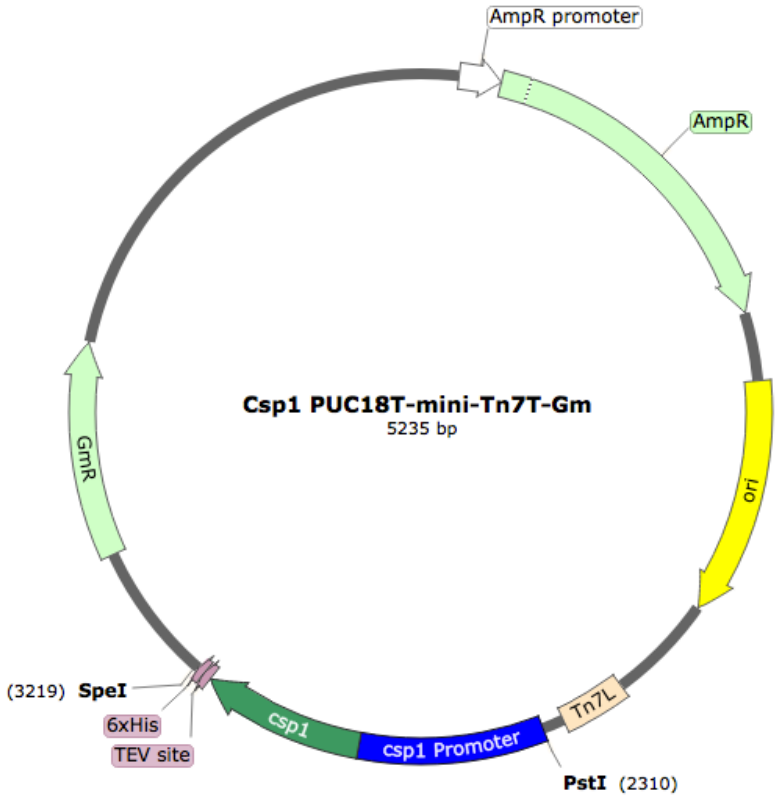

Figure 5: Csp1 pUC18T-mini-Tn7T-Gm complement vector map. Including the restriction digest sites, the gentamicin resistance gene, the ampicillin resistance gene, the TN7L transposon sequence, the arabinose promoter, origin of replication, 6x Histidine tag and TEV cleavage site.

Table 3: Primers used to create *csp1* complement vector.

Primer	Sequence (5'-3')
C-PstI-Csp1-F	CTATACACTGCAGAGCACCGGCTGATGATCCAT
C-SpeI-Csp1-R	TATAGACTAGTTCAGTGGTGGTGGTGGTGGTGG GACTGAAAATACAGGTTTTCGGCAGCAGCGGCC GGCAACAACGGCCGAC

Biparental Conjugation: *P. aeruginosa* PAO1 strain and the mutant vector were grown overnight at 37 °C in a 5 mL test tube with LB media (10 g/l tryptone, 5 g/l yeast extract and 10 g/l NaCl) supplemented with the appropriate antibiotics. 0.2 mL of each culture were added to a microcentrifuge tube containing 1.2 mL of pre warm LB media, which was centrifuged for 2 min at 7,000 xg. The supernatant was discarded, the cell pellet resuspended in 1 mL of LB media and centrifuged for 2 min at 7,000 xg. The supernatant was discarded and the cell pellet resusupended in 50 µL LB media, which was then transferred to a 13-mm cellulose filter placed in LB agar and incubated at 37 °C for 5 h. The filter was then placed in a microcentrifuge tube with 0.2 mL of 0.9% NaCl and vortexed for 30 s. The solution was plated in LB agar containing the proper antibiotic, incubated at 37 °C for 24 h and the colonies were screened by PCR (27).

Protein Expression: Bacteria were grown in 2x YT media supplemented with 100 µg/ml ampicillin at 37 °C for 6 h. The cells were grown during 20 h at 20ºC in ZYP-505 autoinduction media supplemented with 0.05% arabinose and 100 µg/ml ampicillin (29), pelleted by centrifugation for 10 min at 6,000 xg, washed with 100mM KCl, 25mM Tris-HCl (pH 7.0), pelleted under the same conditions and stored at -80 °C until use.

Protein Purification: Cell pellets were resuspended in 4 volumes of 50 mM Tris (pH 7.5) and 300 mM NaCl. Cells were disrupted utilizing the Sonic Dismembrator Model 100 at 6 times for 30 s at power 8 (Fisher Scientific). Cell debris was removed by centrifugation at 15,000 xg for 30 min. The supernatant was loaded to a pre-equilibrated Ni-NTA His-tag column (1mL per 40mg of protein). The column was washed with 10 volumes of 50 mM, Tris (pH 7.5), 300 mM NaCl buffer with increasing concentrations of imidazole (5, 20 and 150 mM). The His-tagged protein was

eluted with 10 volumes of 300 mM imidazole, 50 mM Tris (pH 7.5), 300 mM NaCl. The buffer was exchanged to 2mM EDTA, 1 mM DTT, 50 mM Tris (pH 7.5), 200 mM NaCl by filtration utilizing 10 kDa molecular weight cut-off Centricon (Millipore). This step was repeated until the imidazole concentration dropped below 2 mM. Protein was stored at -20°C in 20% glycerol.

Protein Quantification: Protein concentrations were determined in accordance to Bradford (30). 10 µl protein samples and bovine serum albumin (BSA) standards (0, 5, and 10 µg) were mixed and incubated with 1000 µl Coomassie Reagent for 10 min at RT. Thereafter, absorbance was measured at 595 nm. Protein standards were obtained by diluting a 1 mg/ml stock solution of BSA. Linear regression was used to determine the protein concentration of each sample.

SDS PAGE Electrophoresis: One-dimensional SDS polyacrylamide electrophoresis (SDS-PAGE) was carried on 10% SDS polyacrylamide gels using the Mini-PROTEAN 3 electrophoresis module (Bio-Rad). Protein samples were mixed with 6X Laemmli sample buffer (375 mM Tris-HCl pH 6.8, 50% Glycerol, 9% SDS, 0.03% Bromophenol Blue, β- Mercaptoethanol 5%) and heated at 95°C for 5 min. Electrophoresis was run at 20 mA for 60 min. Proteins were stained using Coomassie brilliant blue. Protein expression was tested by immunostaining Western-blots using rabbit anti-(His)6 polyclonal primary antibody and goat anti-rabbit IgG secondary antibody (GenScript, Piscataway, NJ) (31).

Growth of P. aeruginosa under stress conditions: *P. aeruginosa* PAO1 bacteria were grown in 2x YT media (16 g/l tryptone, 10 g/l yeast extract and 5 g/l NaCl) at 37 °C until an OD_{600} of 1.5. Cells were then divided in 5ml samples and treated with different metals (2 mM $CuSO_2$, 4

mM$CuSO_4$, 2 mM $FeCl_3$, 2 mM $ZnCl_2$) or 100 µM tert-*butyl* hydroperoxide (TBHP). The treated samples were then incubated at 37 °C for 1 h, 1 mL of the treated samples was mixed with one volume of RNA protect bacteria reagent (Qiagen). Cells were centrifuged at 5,000 xg for 10 min and after discarding the supernatant stored at -80 °C.

RNA Extraction, DNAse Treatment and RNA Cleaning: RNA was extracted following the Qiagen RNeasy mini kit protocol. The RNA concentration was then measured utilizing a NanoDrop 2000c spectrophotometer (Thermo Fisher). The RNA sample was treated with DNase (1 unit/ 5 µg of RNA) (New England Bio Labs). Samples were incubated for 40 min at 37°C. One volume of Phenol:Choloroform:Isoamyl alcohol (25:24:1) was added to the treated RNA and centrifuged at 14,000 xg for 5 min. The aqueous phase was recovered and 2.5 volumes of Ethanol 100% was added, incubated for 1h at -20°C and centrifuged at 14,000 xg for 5 min. The supernatant was discarded, the pellet resuspended in Ethanol 70% and centrifuged at 14,000 xg for 2 min. The pellet was then resuspend in water and the RNA concentration measured in a NanoDrop spectrophotometer.

cDNA Synthesis: cDNA synthesis was achieved following Thermo Scientific RevertAid First Strand cDNA synthesis kit protocol utilizing random hexamer primers.

RT-qPCR: Purified cDNA (1 µg), internal forward and reverse primers (Table 2) were added to appropriate amount of FastStart Essential DNA Green Master mix from Roche.

copA1 and *copA2* genes were used as positive and negative controls for expression under Cu^{+2} stress conditions, respectively. *PA4268* (30S ribosomal gene) was used as housekeeping gene. The

samples were loaded to a 96 well plate, and run in a LightCycler® 96 System (Roche) with the following settings: the RT-qPCR involved a preincubation at 95 °C for 10 min, a two-step amplification repeated 45 times with denaturation at 95 °C for 10 s followed by elongation at 65 °C for 30 s, and a final a cooling step at 37 °C for 30 s. Utilizing *PA4268* as a reference gene relative expression for *csp1, copA1, copA2* and *cueR* was measured following the following formula.

$$\frac{E_T^{Cq_{T,\,cal}-Cq_T}}{E_R^{Cq_{R,\,cal}-Cq_R}}$$

- E_T = Amplification efficiency of the target gene
- E_R = Amplification efficiency of the reference gene
- Cq_T = Quantification cycle of the target gene
- Cq_R = Quantification cycle of the reference gene
- Cal = Study Calibrator

Table 4: RT-qPCR primers

Primer	Sequence (5'-3')
qCsp1-F	GAGTCCAGCAGGGAACAA
qCsp1-R	AACAACGGCCGACAGG
qCopA1-F	GAAACGGTGCTGGCGAAGAT
qCopA1-R	TTAACCAGGGCCTGCTCCAG
qCopA2-F	CAGCAGGACGATGAGCAGGA
qCopA2-R	CTGCTCACCGGCGAGTACCT
qPA4268-F	GCAAAACTGCCCGCAACGTC
qPA4268-R	TACACGACCGCCACGGATCA
qCueR-F	TCCGTTACTACG AGTCCATCG
qCueR-R	GTGCTGAGCTCCTCGATCTT

III. Results

Cu^{+}-dependent gene expression

Previously studied metallothioneins have been shown to be over expressed under stress conditions (24,32). In order to study the role of Csp1 in resistance to transition metals, RT-qPCR was performed to analyze the transcription levels of *csp1, copA1, copA2 and cueR* under different stress conditions. CopA1 and CopA2 and CueR are major players in Cu^{+} homeostasis, and thus were used as internal controls of the experiment. CopA1 participates in metal detoxification and CopA2 in protein metalation. CueR is a key Cu^{+} sensor and transcriptional regulator. As seen in Figure 4A, treatment with 2 mM and 4 mM Cu^{+2} does not affect the expression level of *csp1*. Moreover, absolute expression levels are low (data not shown). We did observe increased expression of *copA1* with respect to untreated samples. These results confirm that CopA1 plays a major role in Cu^{+1} detoxification, unlike Csp1 and CopA2. When exposed to oxidative stress in the form of TBHP 100 μM, *copA1* expression is repressed (Figure 6C). Meanwhile, when exposed to other transition metals, we did not observe any major increases in expression for any of the genes assayed (Figure 6B). These results suggest that the regulation of Csp1 under Cu^{+1} stress occurs at a post-transcriptional level. Thus, we attempted to the role of Csp1 through functional characterization at the protein level.

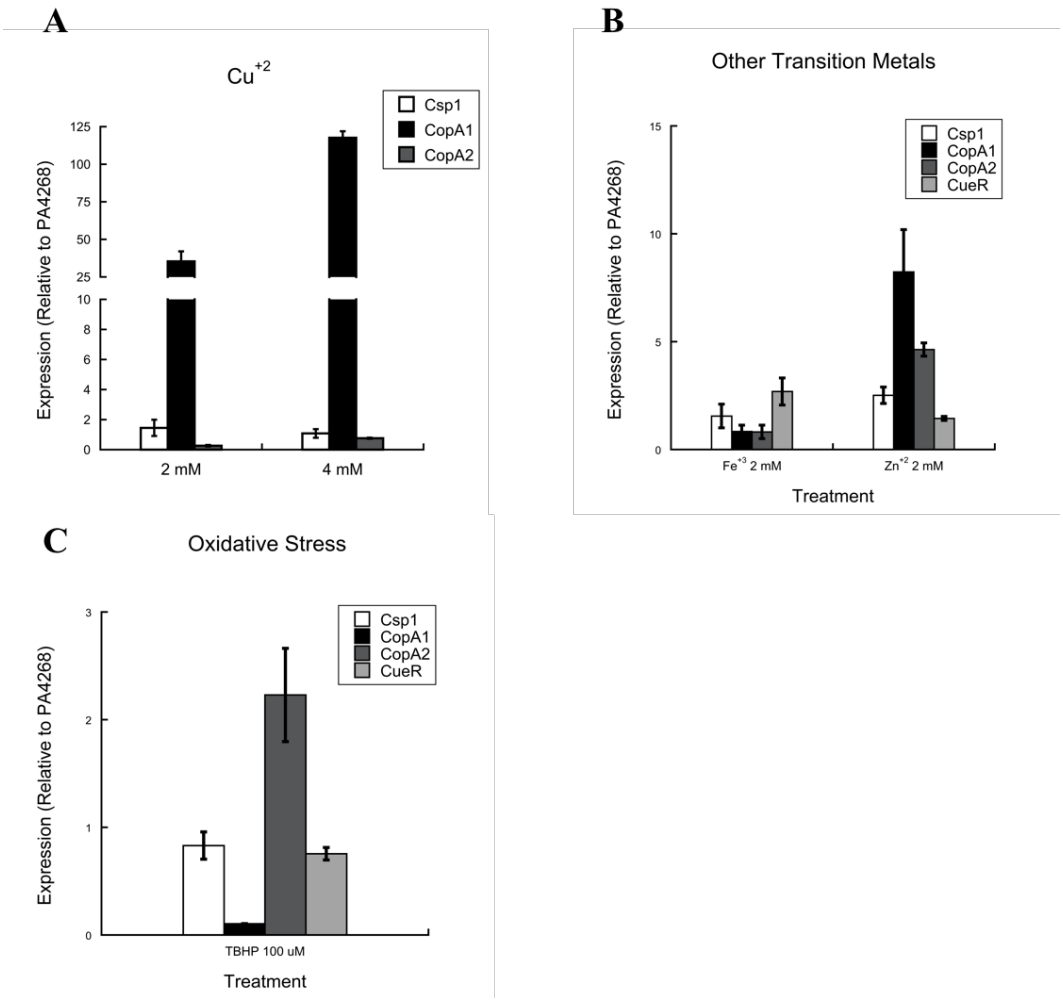

Figure 4: Relative expression of *csp1, copA1, copA2* and *cueR* in respect to P*A4268*. **A.** Relative expression of *csp1, copA1* and *copA2* under Cu^{+2} stress. **B.** Relative expression of *csp1, copA1, copA2* and *cueR* under transition metal stress. **C.** Relative expression of *csp1, copA1, copA2* and *cueR* under oxidative stress.

Generation of csp1 mutant and complemented strains

Cloning and Transformation: The transposon mutant collection of *P. aeruginosa* does not harbor a mutant strain for Csp1. To study the biological role of Csp1 the generation of a mutant strain became imperative. To achieve this goal a truncated version of the gene was cloned into a plasmid for homologous recombination in WT *P. aeruginosa.* The vector chosen to perform this task was the pCHESIΩKm vector. Successful cloning was demonstrated by performing a restriction digest utilizing the specific sites added at the beginning (KpnI) and end (XbaI) of the PCR insert. Double

digestion, as shown in Figure 7, confirmed a band for the pCHESIΩKm vector of around 5.6kb and a second band for the Csp1 gene fragment insert of around 370 bp.

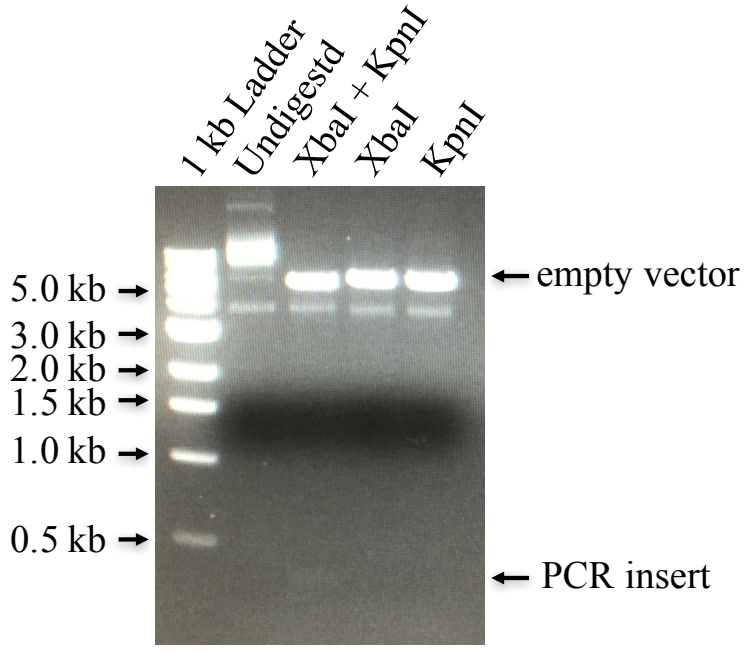

Figure 7: Agarose gel electrophoresis of restriction digest of Csp1::pCHESIΩKm mutant plasmid.

Insertion of Csp1::pCHESIΩKm in P. aeruginosa genome: Several attempts were carried out to introduce the truncated form of Csp1 into the *P. aeruginosa* genome using biparental conjugation with *E. coli* S17-1 as the donor strain. Colony PCR was performed using two sets of primers. As positive control, the primers used for cloning the gragment were employed; then, to test for the positive insertion a set of primers that amplify the whole gene were used. If the truncated gene had successfully integrated itself into the WT genome, the second set of primers would not amplify. As seen in Figure 8, both set of plasmid yield amplicons from antibiotic resistant colonies contained. This experimental constraint has not been solved, and is probably due to transitory recombination.

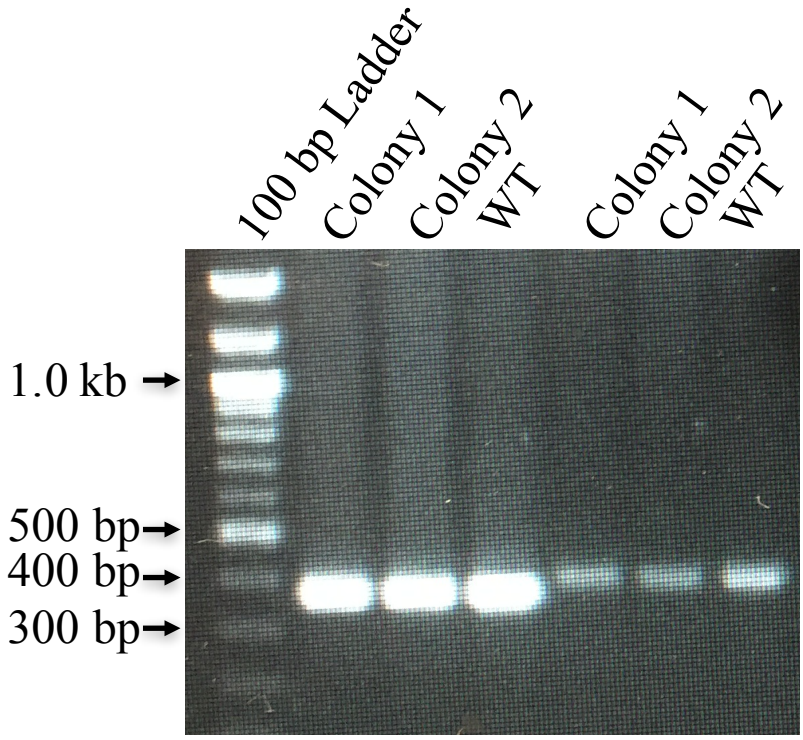

Figure 8: Agarose gel electrophoresis of colony PCR products from biparental conjugation. Lane 1 denotes the ladder. Lanes 2, 3 and 4 show positive control for the PCR amplified region of the gene of two antibiotic resistant mutants and WT PAO1. Lanes 5, 6 and 7 show the PCR amplified region of the gene of two antibiotic resistant mutants and WT PAO1.

Cloning and Transformation of Complement Vector: In order to gain insight into the role of Csp1, complementation of the mutant should also be tested. To this end, we initiated the construction of necessary vector. We used PUC18T-miniTN7T-Gm vector, to insert a single copy of a gene into the genome using the single attTn7 sites located next to the *glsm* gene. A 500 bp region upstream of the gene, containing the promoter region, RBS and transcription start site was cloned. Restriction digest was subsequently performed with the specific restriction sites added at the start (PstI) and end (SpeI) of the PCR product. The double digest seen in lane 5 of Figure 9, confirmed the proper addition of the PCR product by showing a band for the PUC18T-miniTN7T-Gm vector of around 4.3kb and a band for the *csp1* gene fraction insert of around 931bp.

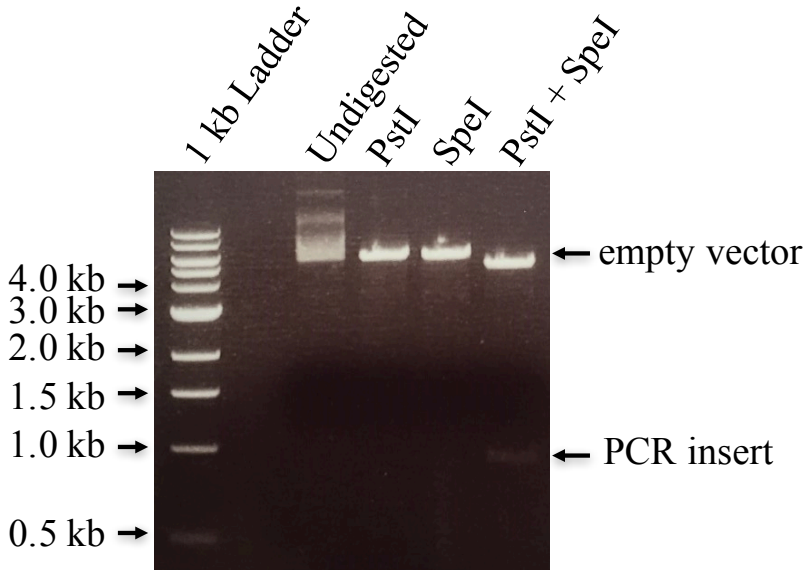

Figure 9: Agarose gel electrophoresis of restriction digest of Csp1::PUC18T-miniTN7T-Gm complement plasmid.

Protein Expression and Purification

Cloning and Transformation of Expression Vector: To study the metal binding ability of the Csp1, the protein was expressed in *E. coli* under the control of an arabinose-inducible promoter. The expression clone included a copy of *csp1*, a TEV cleavage site and a Histidine tag for affinity purification (Fig. 4). Correct insertion into the pBAD Topo expression vector was verified by performing a restriction digest using the restriction sites KpnI and EcoRI. Double digestion (lane 5 of Figure 10A) confirmed correct cloning by showing the band for the pBAD expression vector of around 4.1 kb and a band for the Csp1 gene insert of around 470 bp. As shown in Figure 10B, the sequence of the gene was verified through automated sequencing.

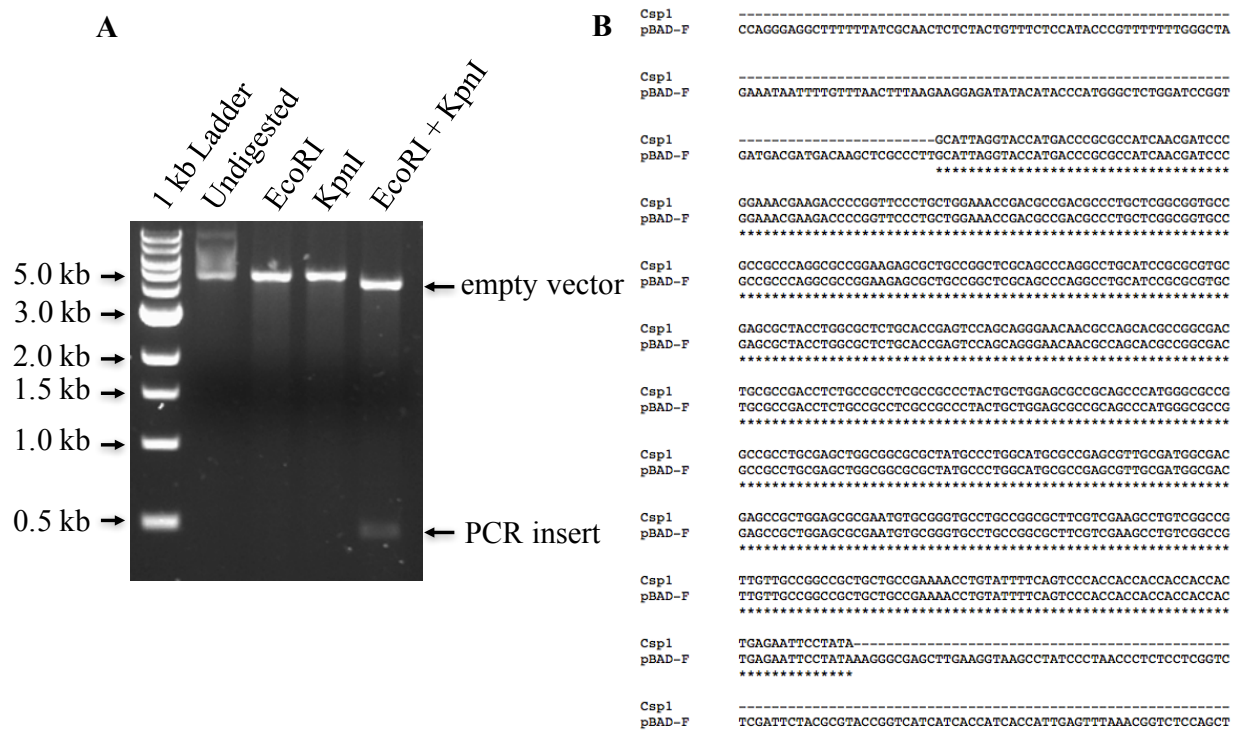

Figure 10: Csp1 insertion into pBAD expression vector. **A.** Agarose gel electrophoresis of restriction digest of Csp1::pBAD expression plasmid. **B.** Automated sequencing results. Top row shows Csp1 gene and bottom row shows the Csp1 gene inserted in the pBAD vector without any mutations in the gene.

Heterologous expression: Small-scale expression was performed to optimize the induction conditions to express Csp1 in *E. coli* LMG194 using arabinose as inducer. LMG-194 cells containing the Csp1:pBAD construct where grown in 2xYT media and Autoinduction Media (AIM), which were treated with different amounts of arabinose and the expression levels where analyzed using TEV:His as control. Immunostaining of different fractions is depicted in Figure 11. Csp1 was successfully expressed under all conditions, with the highest yields in AIM media.

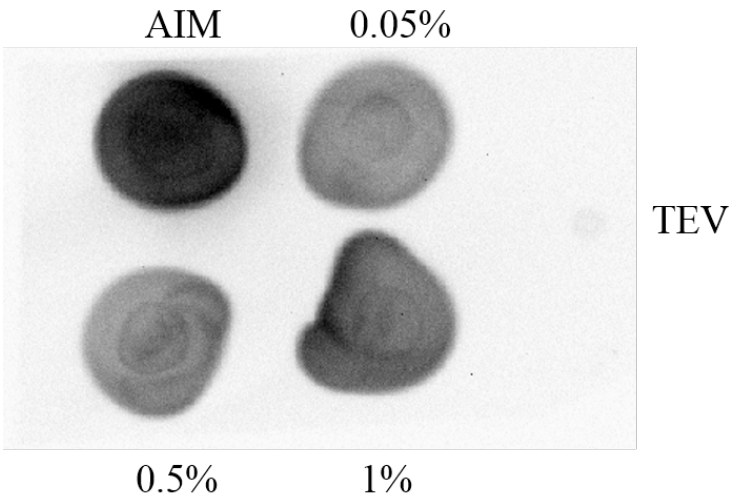

Figure 11: Immunostaining of protein expression test of Csp1::pBAD plasmid. TEV (2µg) is the positive control. Percentages show the amount of Arabinose used to induce the cells, while AIM refers to Autoinduction media (See Methods).

Protein Purification: Csp1-His tagged protein was affinity-purified a Ni-NTA column, that binds 6xHis tag located in the carboxylate terminal of the protein. Figure 12 shows the different steps of purification. Column was washed with different concentrations of imidazole (5 and 20 mM) to remove non-specific binging. Protein was eluted in the 150mM imidazole fractions as well as in the 300mM imidazole ones.

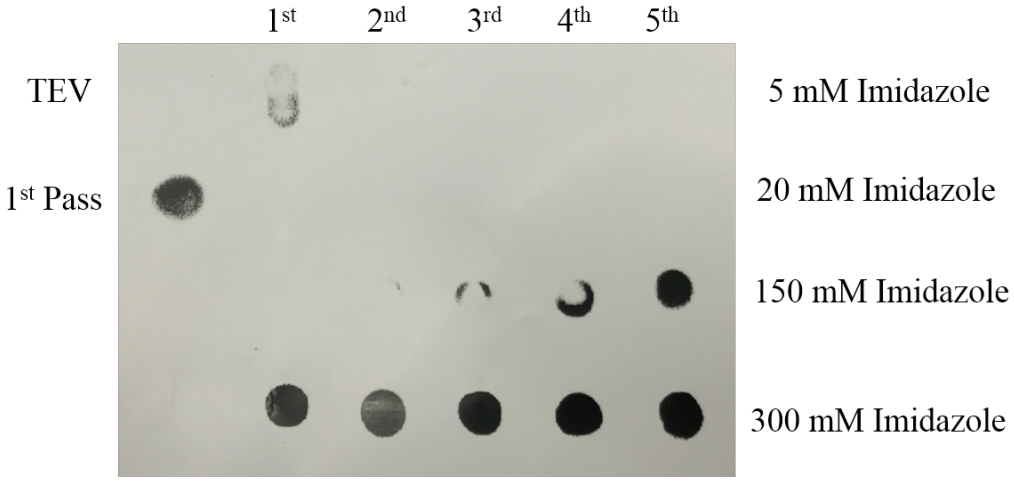

Figure 12: Immunostaining of protein purification. Top row shows the fraction while the right column shows the percentage of imidazole used to elute that fraction.

Purity of the eluted protein was assessed with SDS-PAGE. Csp1 has a monomeric weight of 12.5 kDa. As seen in Figure 13 there are no clear bands in that region of the gel for any of the eluted fractions with 150 mM and 300 mM imidazole. Then results suggest that the protein was not purified as a monomer, but in the form of different homomeric complexes. The bands in the 25 kDa and 37 kDa area at lanes 6 and 7 support this observation.

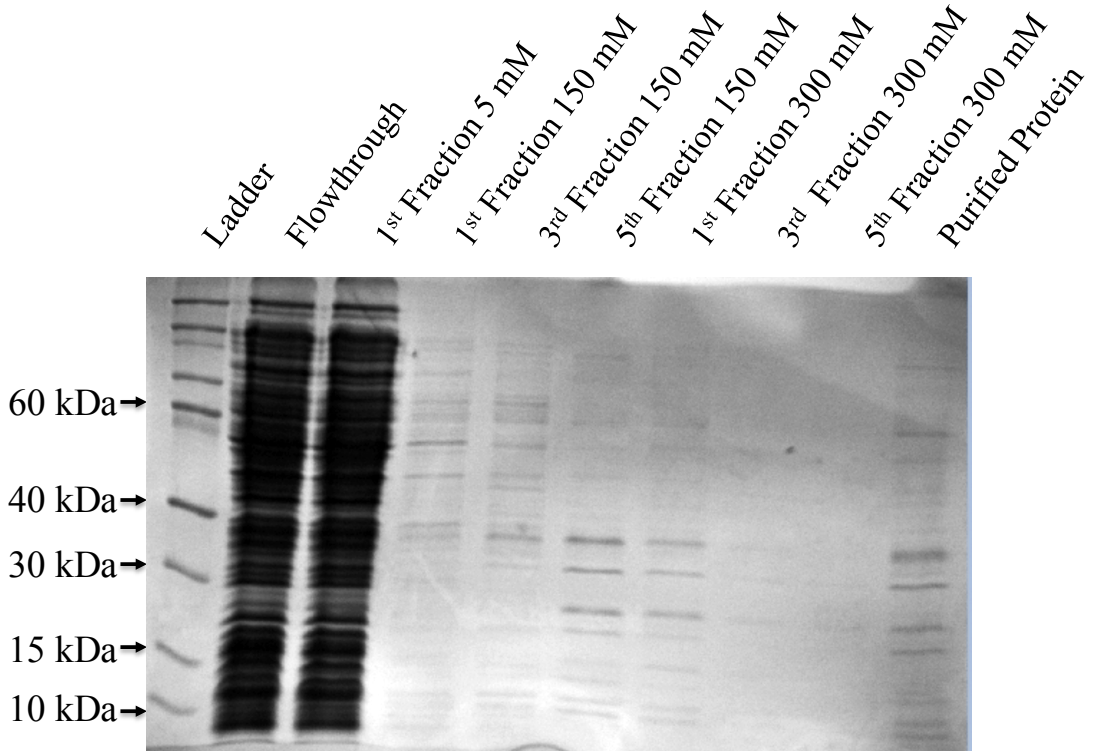

Figure13: SDS PAGE with Coomassie staining of eluted fractions. Lane 1 is the ladder. Lane 2 represent the flow through. Lane 3 shows the first wash with 5mM imidazole. Lanes 4, 5 and 6 show 1st, 3rd and 5th fraction eluted with 150mM imidazole. Lanes 7, 8 and 9 show 1st, 3rd and 5th fraction eluted with 300mM imidazole. Lane 10 shows purified protein from all the 150mM imidazole fractions.

IV. Discussion

Due to Cu^{+} ability to damage cellular machinery through Fenton-like chemistry, it has been a common hypothesis that a system to limit free soluble Cu^{+1} ions is necessary for cellular survival. Until recently a Cu^{+1} storage protein in gram-negative bacteria remained elusive (25). The discovery of a such a protein propelled us to study its orthologue, Csp1, in *P. aeruginosa,* a gram-negative bacterium with the ability to quickly develop antibiotic resistance and survive in extreme environments. Our goal was to determine whether the *P. aeruginosa* Csp1 protein, functions as a Cu^{+1} storage compartment. attempted. Through our results, we were unable to show the importance of Csp1 for Cu^{+1} detoxification. The ability of Csp1 in *P. aeruginosa* to bind and store Cu^{+1}, as well as its importance for cell viability, are still under investigation.

Previous studies have shown up-regulation of metallothioneins under excess of transition metals and oxidative stress (24,32,33). As seen in Figure 6A, under excess Cu^{+2} the transcript levels of csp1 remained constant, suggesting Csp1 might not play a role in Cu homeostasis. Looking for alternative roles of Csp1, we also test the effect of other heavy metals and redox-stress conditions on its expression levels, however none of the treatments cause a change in the expression profile of csp1 (fig 6B and C). To validate the results, expression levels of CopA1 and CopA2, two Cu^{+1} efflux P-type ATPase pumps, previously described as involved in Cu^{+1} detoxification and metallation of cytochrome c oxidase, respectively were tested (12). As expected, the expression levels of CopA1, markedly increased in a copper-dependent manner while the expression of CopA2 is only stimulated by oxidative stress.

One of the major obstacles in this project was not being able to obtain a *P. aeruginosa* Csp1 mutant and complement. As seen in Figure 7 and 10, the Csp1::pCHESIΩKm and

Csp1::pUC18T plasmids capable of making the mutant and complement strains were created in *E. coli,* but issues arrived when trying to integrate these vectors into *P. aeruginosa*. To form the mutant, pCHESIΩKm vector was utilized, as this vector is capable of performing homologous recombination through biparental conjugation. The method by which this plasmid creates a mutant is interrupting the gene of interest by introducing itself in the middle of the sequence, thus limiting any ability of the bacteria to produce the gene. Although multiple biparental conjugations were performed under different conditions, colony PCR never showed a full positive result for the Csp1 mutant. This issue might have been created by transitory recombination, where there are two genes present in the cell: the WT genome and the Csp1 mutant gene. This transitory recombination allowed for WT bacteria to gain antibiotic selection and show amplification in colonies that had been screened by antibiotic. To overcome this issue, we suggest the use of another plasmid capable of performing recombination in a similar manner to pCHESIΩKm, as other laboratories have reported similar problems with their pCHESI strains, or utilize commercial kits to create a mutant of Csp1. The inability to produce a viable mutant restricted our capability of creating a proper Csp1 complement to study the importance of Csp1 for Cu^{+1} detoxification and cell viability.

Based on Csp1's sequence similarity to the previously characterized orthologue we pursued the idea of Cu^{+1} binding and storage. Unfortunately, towards the end of the project we ran into problems purifying the protein. As observed in the immunostaining dot blot in Figure 12, the protein was expected to be eluted in the 300 mM imidazole fractions. However, in the Coomassie stained gel in Figure 13 there are no protein bands for the 150 mM imidazole or 300 mM imidazole fractions around the 12.5 kDa area where Csp1 is expected to separate. To determine where Csp1 is eluting, it would be beneficial to run a Western Blot where we could observe specifically where our protein is congregating. Csp1, a tetramer in non-reducing environments, may have separated

to other weight bands if it was unable to be denatured fully. In the gel there are bands in the 25 kDa and 37.5 kDa, which might be composed of Csp1 dimmers or trimmers, but in order to confirm this theory immunostaining is needed. Due to time constrains and difficulty purifying the protein the Cu^{+}-Csp1 binding analysis were not performed.

The role of Csp1 in Cu^{+} homeostasis remains elusive. Our RT-qPCR results show that Csp1 might not be involved in Cu^{+} homeostasis. However, these results do not rule out a possible role for Csp1 in Cu^{+1} detoxification due to the high number of Cu^{+1} ions that it can possibly bind. Suggesting that regulation of Csp1 under Cu^{+} stress might occur at a post-transcription. Nonetheless, a solid path to follow has been laid down to further investigate its role. Future studies of Csp1 should start by looking at alternative protocols to promote the homologous recombination of the plasmid Csp1::pCHESIΩKm in order to obtain the mutant strain. Once obtained, plasmid Csp1::pUC18T can be used to complement the mutant strain. This should be done in tandem with the Csp1::pBAD plasmid obtained here to purify the Csp1 His-tagged protein to determine its ability to bind Cu^{+1}. The completion of these experiments would give us a better and more detailed understanding of the role of Csp1 in *P. aeruginosa*.

Reference

1. Paul B. Tchounwou, C. G. Y., Anita K. Patlolla, Dwayne J. Sutton. (2012) Heavy Metals Toxicity and the Environment. . *Molecular, clinical and environmental toxicology* **101**, 133-164
2. Oves M, S. K. M., Huda Qari A1,3, Nadeen Felemban M and Almeelbi T. (2016) Heavy Metals: Biological Importance and Detoxification Strategies. *Journal of Bioremediation & Biodegradation* **7**
3. Brunori, M., Giuffre, A., and Sarti, P. (2005) Cytochrome c oxidase, ligands and electrons. *Journal Inorganic Biochemestry* **99**, 324-336
4. Desideri, A., and Falconi, M. (2003) Prokaryotic Cu,Zn superoxide dismutases. *Biochemical Society Transaction* **31**, 1322-1325
5. Valko, M., Morris, H., and Cronin, M. T. (2005) Metals, toxicity and oxidative stress. *Curr Med Chem* **12**, 1161-1208
6. Rae, T. D., Schmidt, P. J., Pufahl, R. A., Culotta, V. C., and O'Halloran, T. V. (1999) Undetectable intracellular free copper: the requirement of a copper chaperone for superoxide dismutase. *Science* **284**, 805-808
7. Lutsenko, S., Barnes, N. L., Bartee, M. Y., and Dmitriev, O. Y. (2007) Function and regulation of human copper-transporting ATPases. *Physiological Reviews* **87**, 1011-1046
8. Vulpe, C., Levinson, B., Whitney, S., Packman, S., and Gitschier, J. (1993) Isolation of a candidate gene for Menkes disease and evidence that it encodes a copper-transporting ATPase. *Nat Genet* **3**, 7-13
9. Tanzi, R. E., Petrukhin, K., Chernov, I., Pellequer, J. L., Wasco, W., Ross, B., Romano, D. M., Parano, E., Pavone, L., Brzustowicz, L. M., and et al. (1993) The Wilson disease gene is a copper transporting ATPase with homology to the Menkes disease gene. *Nat Genet* **5**, 344-350
10. de Bie, P., Muller, P., Wijmenga, C., and Klomp, L. W. (2007) Molecular pathogenesis of Wilson and Menkes disease: correlation of mutations with molecular defects and disease phenotypes. *Journal of Medical Genetics* **44**, 673-688
11. Schwan, W. R., Warrener, P., Keunz, E., Stover, C. K., and Folger, K. R. (2005) Mutations in the cueA gene encoding a copper homeostasis P-type ATPase reduce the pathogenicity of Pseudomonas aeruginosa in mice. *Int J Med Microbiol* **295**, 237-242
12. Gonzalez-Guerrero, M., Raimunda, D., Cheng, X., and Arguello, J. M. (2010) Distinct functional roles of homologous Cu+ efflux ATPases in Pseudomonas aeruginosa. *Molecular Microbiology* **78**, 1246-1258
13. Arguello, J. M., Raimunda, D., and Padilla-Benavides, T. (2013) Mechanisms of copper homeostasis in bacteria. *Frontiers in Cellular and Infection Microbiology* **3**, 73
14. Ekici, S., Yang, H., Koch, H. G., and Daldal, F. (2012) Novel transporter required for biogenesis of cbb3-type cytochrome c oxidase in Rhodobacter capsulatus. *MBio* **3**
15. Gonzalez-Guerrero, M., and Arguello, J. M. (2008) Mechanism of Cu+-transporting ATPases: soluble Cu+ chaperones directly transfer Cu+ to transmembrane transport sites. *Proceedings of the National Academy of Sciences* **105**, 5992-5997
16. Raimunda, D., Gonzalez-Guerrero, M., Leeber, B. W., 3rd, and Arguello, J. M. (2011) The transport mechanism of bacterial Cu+-ATPases: distinct efflux rates adapted to different function. *Biometals* **24**, 467-475
17. Hancock, R. E., and Speert, D. P. (2000) Antibiotic resistance in Pseudomonas aeruginosa: mechanisms and impact on treatment. *Drug Resistance Updates* **3**, 247-255

18. Hardalo, C., and Edberg, S. C. (1997) Pseudomonas aeruginosa: assessment of risk from drinking water. *Critical Reviews in Microbiology* **23**, 47-75
19. (2001) National Nosocomial Infections Surveillance (NNIS) System Report, Data Summary from January 1992-June 2001, issued August 2001. *Am J Infect Control* **29**, 404-421
20. Organization, W. H. (2017) Global priority list of antibiotic-resistant bacteria to guide research, discovery, and development of new antibiotics.
21. Arguello, J. M., Patel, S. J., and Quintana, J. (2016) Bacterial Cu(+)-ATPases: models for molecular structure-function studies. *Metallomics* **8**, 906-914
22. Calderone, V., Dolderer, B., Hartmann, H. J., Echner, H., Luchinat, C., Del Bianco, C., Mangani, S., and Weser, U. (2005) The crystal structure of yeast copper thionein: the solution of a long-lasting enigma. *Proceedings of the National Academy of Sciences* **102**, 51-56
23. Reddie, K. G., and Carroll, K. S. (2008) Expanding the functional diversity of proteins through cysteine oxidation. *Curr Opin Chem Biol* **12**, 746-754
24. Gold, B., Deng, H., Bryk, R., Vargas, D., Eliezer, D., Roberts, J., Jiang, X., and Nathan, C. (2008) Identification of a copper-binding metallothionein in pathogenic mycobacteria. *Nature Chemical Biology* **4**, 609-616
25. Vita, N., Platsaki, S., Basle, A., Allen, S. J., Paterson, N. G., Crombie, A. T., Murrell, J. C., Waldron, K. J., and Dennison, C. (2015) A four-helix bundle stores copper for methane oxidation. *Nature* **525**, 140-143
26. Winsor, G. L., Griffiths, E. J., Lo, R., Dhillon, B. K., Shay, J. A., and Brinkman, F. S. (2016) Enhanced annotations and features for comparing thousands of Pseudomonas genomes in the Pseudomonas genome database. *Nucleic Acids Res* **44**, D646-653
27. Llamas, M. A., Rodriguez-Herva, J. J., Hancock, R. E., Bitter, W., Tommassen, J., and Ramos, J. L. (2003) Role of Pseudomonas putida tol-oprL gene products in uptake of solutes through the cytoplasmic membrane. *Journal of Bacteriology* **185**, 4707-4716
28. Choi, K. H., and Schweizer, H. P. (2006) mini-Tn7 insertion in bacteria with single attTn7 sites: example Pseudomonas aeruginosa. *Nature Protocol* **1**, 153-161
29. Studier, F. W. (2005) Protein production by auto-induction in high density shaking cultures. *Protein Expr Purif* **41**, 207-234
30. Bradford, M. M. (1976) A rapid and sensitive method for the quantitation of microgram quantities of protein utilizing the principle of protein-dye binding. *Analytical Biochemestry* **72**, 248-254
31. Raimunda, D., Long, J. E., Sassetti, C. M., and Arguello, J. M. (2012) Role in metal homeostasis of CtpD, a Co(2)(+) transporting P(1B4)-ATPase of Mycobacterium smegmatis. *Mol Microbiol* **84**, 1139-1149
32. Man, A. K., and Woo, N. Y. (2008) Upregulation of metallothionein and glucose-6-phosphate dehydrogenase expression in silver sea bream, Sparus sarba exposed to sublethal levels of cadmium. *Aquatic Toxicology* **89**, 214-221
33. Sato, M., and Bremner, I. (1993) Oxygen free radicals and metallothionein. *Free Radic Biol Med* **14**, 325-337